Films of 2-methylbenzimidazole perchlorate $C_8H_8N_2$—$HClO_4$: phase transformations, crystal structure and dielectric properties

© E.V. Balashova, A.A. Levin, B.B. Krichevtsov

Ioffe Institute, St. Petersburg, Russia
E-mail: balashova@mail.ioffe.ru

Films of the semi-organic compound 2-methylbenzimidazole perchlorate, MBI·HClO4, were grown by evaporation at room temperature from an aqueous solution of MBI·HClO4 on quartz glass and sapphire substrates. The results of temperature changes in capacitance, dielectric losses and conductivity of films with simultaneous registration of phase transformations using a polarizing microscope, as well as the results of X-ray diffraction measurements of the crystal structure of MBI·HClO4 films before and after melting and crystallization are presented.

Keywords: phase transformations, crystal structure, dielectric properties, ionic liquids, semi-organic crystals.

Much attention is currently being paid to the search for and study of new semi-organic crystals and films that may be used to obtain multifunctional materials for energy harvesting and produce flexible materials for electronics, sensors of various fields, piezoelectric elements, nonlinear optical devices, membranes of fuel cells for hydrogen energy, biomedical and biotechnological devices, etc. Of particular interest in this context are crystals and films synthesized from aqueous solutions of perchloric acid ($HClO_4$) with various organic components, since they can exhibit ferroelectric, piezoelectric, and nonlinear optical properties and form plastic intermediate phases [1–4].

We have recently grown new crystals of 2-methylbenzimidazole perchlorate (MBI·$HClO_4$) [5] at the Ioffe Institute by combining $HClO_4$ and organic molecular ferroelectric 2-methylbenzimidazole $C_8H_8N_2$ (MBI) [6]. Semi-organic MBI·$HClO_4$ crystals have a monoclinic centrosymmetric lattice with space group $P2_1/n$ (14) with four $(C_8H_8N_2)(HClO_4)$ formula units per lattice cell ($Z = 4$). As was demonstrated in calorimetric and dielectric studies of crystals, the MBI·$HClO_4$ melt has the properties of an ionic liquid (IL) at temperatures above melting point $T_{c1}^h = 168.4°C$, and an intermediate solid phase, which differs from the phase manifested at room temperature, emerges at temperatures below $T_{c1}^c = 157.8°C$ [5]. The aim of the present study is to synthesize MBI·$HClO_4$ films on various substrates, compare the crystal structure of films formed from solution and melt, and examine the dielectric properties of films in the course of phase transformations with simultaneous photographic recording of the state and structure of films with a polarizing microscope.

MBI·$HClO_4$ films were first grown by evaporation at room temperature from an aqueous solution of MBI·$HClO_4$ on substrates made of fused quartz and sapphire (Al_2O_3). Such substrates have previously been used to grow films of amino acid ferroelectrics [7]. When the temperature was raised above $T_{c1}^h \approx 426$ K ($153°C$), the MBI·$HClO_4$ film passed into a liquid state, and a film synthesized from melt was obtained as the temperature was subsequently lowered to room levels. In order to perform dielectric measurements, a system of gold interdigital electrodes (IDEs) was formed in advance on sapphire substrates by photolithography. The width of these electrodes was $50 \mu m$, the distance between them was $50 \mu m$, and the number of electrode pairs was $N = 30$. Capacitance C, dielectric losses tgδ, and conductivity G between the IDEs were measured for the obtained structures (MBI·$HClO_4$ film/IDE/Al_2O_3 substrate) within the frequency range of $f = 25 - 10^6$ Hz and the temperature range of $295 - 460$ K with the use of MIT 9216A (Protek Instrument, Gyeonggi-do, Republic of Korea) and E7-20 (MNIPI, Minsk, Belarus) LCR meters and the LabView software package (version 2011, NIST, Gaithersburg, Maryland, United States). Alongside with these dielectric measurements, the film state was monitored with a LaboPol-3 polarizing microscope. The film was imaged in transmitted or reflected light in crossed or parallel polarizers.

X-ray diffraction (XRD) measurements of MBI·$HClO_4$ films before and after melting and crystallization were carried out with a D2 Phaser (Bruker AXS, Germany) X-ray powder diffractometer using CuK_α-radiation at temperature $T_{meas} = 313 \pm 1$ K in the symmetric $\theta - 2\theta$ scanning mode. To determine angular corrections to the measured diffraction patterns, additional measurements were carried out for substrates and films in NaCl powder, the 2θ-angle positions of XRD reflections of which were calibrated against the Si640f powder standard (NIST, United States).

It can be seen from Fig. 1 that all the observed reflections of the film on the quartz glass substrate (samples Nos. 3 and 4) and on the single-crystal (0001) Al_2O_3 substrate (before and after recrystallization) belong to the monoclinic MBI·$HClO_4$ phase (space group $P2_1/n$ (14)) [5]. The
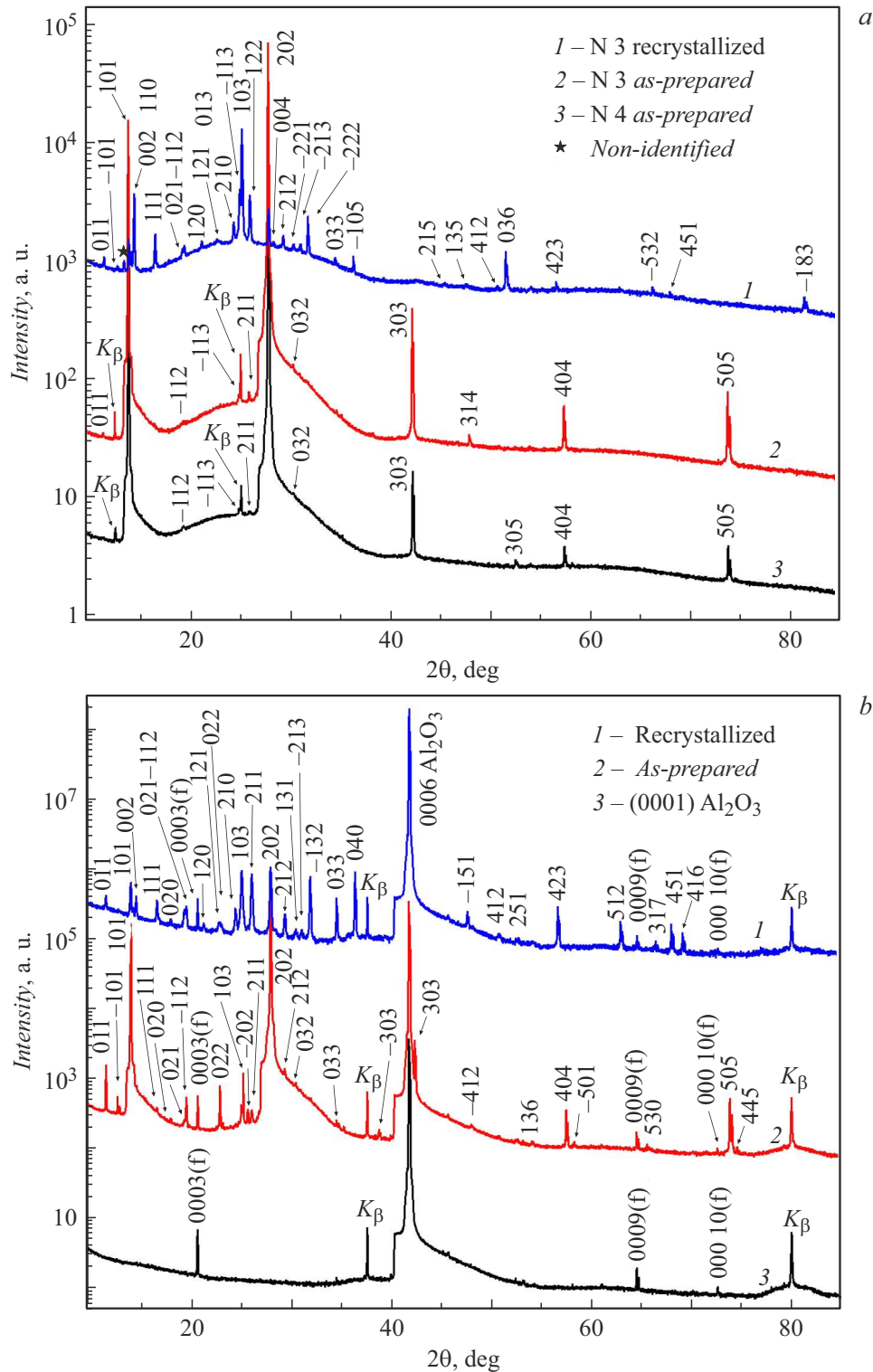
Figure 1. XRD patterns of MBI · HClO$_4$ films on substrates made of fused quartz (SiO$_2$) (*a*) and a single-crystal (0001) Al$_2$O$_3$ wafer (*b*). The XRD pattern of the (0001) Al$_2$O$_3$ substrate without a film is shown in panel *b* for comparison. Miller indices *hkl* of the observed reflections for the MBI · HClO$_4$ film material, which has monoclinic lattice symmetry, and Miller−Bravais indices *hkil* of reflections of the α-Al$_2$O$_3$ substrate with rhombohedral symmetry in the hexagonal frame are indicated in panels *a* and *b*. Symbol „f" in panel *b* denotes symmetry-forbidden reflections (0001) of the Al$_2$O$_3$ substrate. The reflection of an unidentified phase in the film after recrystallization on the SiO$_2$ glass substrate is denoted with an asterisk. Residual strong reflections corresponding to K_β-emission are also indicated.
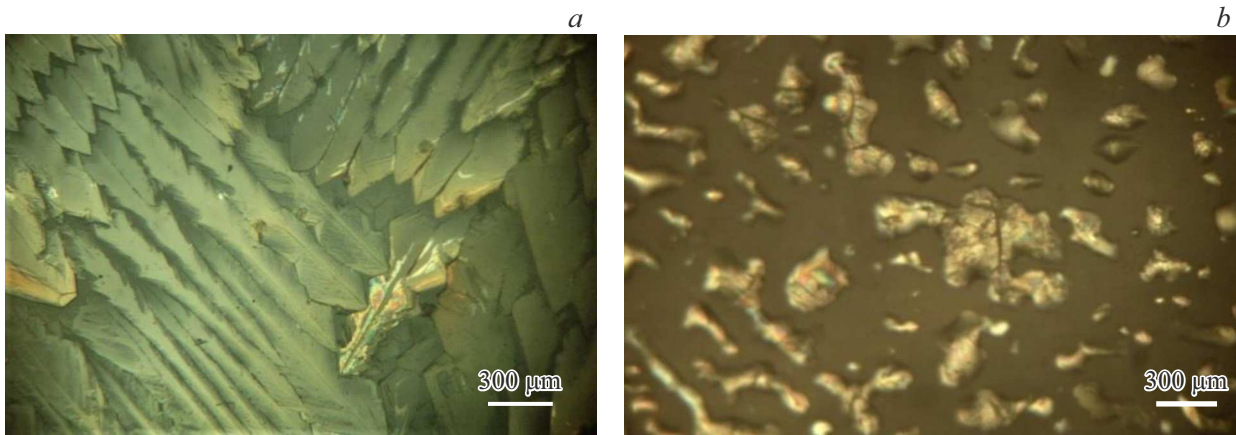
Figure 2. *a* — Polarizing microscope image of the MBI · HClO₄ film in the initial low-temperature phase obtained at temperature $T = 27°$C. The film was grown from solution on the Al₂O₃ substrate at room temperature. *b* — Image of the same film at $T = 38.5°$C obtained after cooling from the MBI · HClO₄ melt.
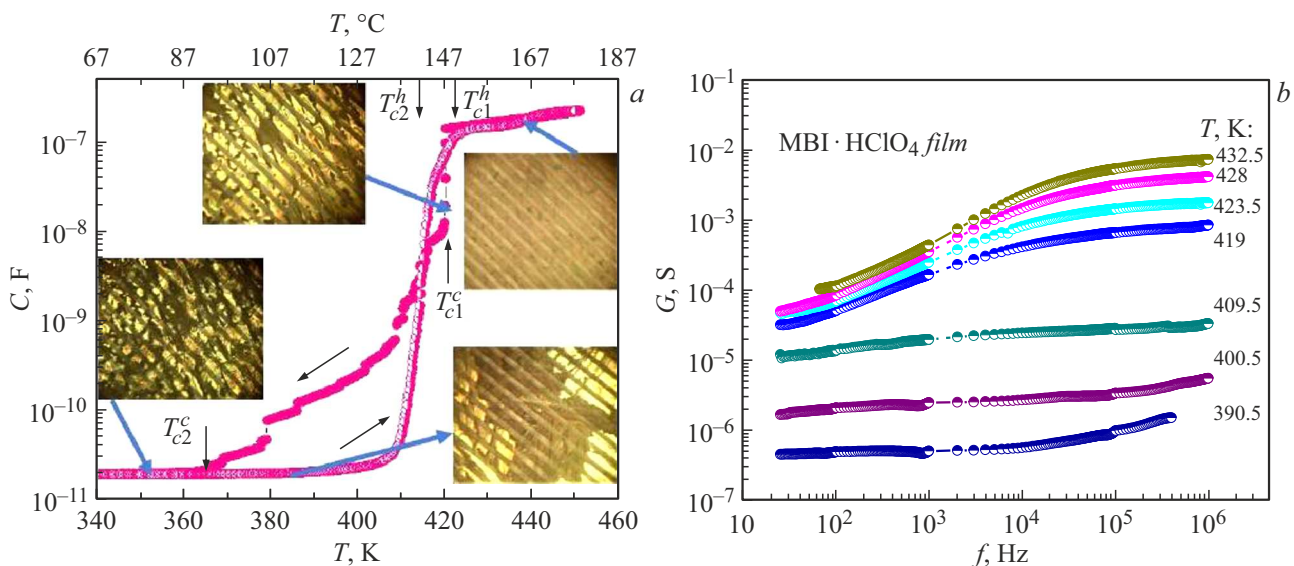
Figure 3. *a* — Temperature dependence of capacitance C of the MBI · HClO₄/IDE/Al₂O₃ structure heated to melting and cooled. The insets show changes in the film structure revealed in a polarization microscope in crossed polarizers. *b* — Frequency dependences of the film conductivity at different temperatures during cooling from melt.

values of parameters (a, b, c, and monoclinicity angle β) and volume (V_{cell}) of the monoclinic lattice cell of crystals and films of MBI · HClO₄ calculated in Celsiz [8] are listed in the table. It is evident that these values are close to each other. Recrystallization leads to a change in volume V_{cell} of the unit cell, which becomes closer to the one observed for MBI · HClO₄ powder [5] prepared by grinding of single crystals.

The results of XRD studies revealed that films grown from an aqueous solution contain ~ 99.9 wt.% of large MBI · HClO₄ crystallites of the same space group $P2_1/n$ (14) as bulk crystals [5] with crystallographic planes ($h0h$) parallel to the film surface (Figs. 1, a, b). This follows from the fact that the observed $h0h$-type MBI · HClO₄ reflections are the most intense and very

narrow, especially in the case of the Al₂O₃ substrate. At the same time, reflections of the other type are very weak (with relative intensities of ~ 0.1% and less), and only a limited number of these reflections is seen. When the ($T_{c1}^h \approx 426$ K (153°C)) film is heated to complete melting with subsequent lowering of the temperature to room levels, MBI · HClO₄ recrystallizes. The $h0h$ reflections grow wider as a result, and a large number of reflections with arbitrary hkl and intensities higher than those observed before recrystallization appear. It may be concluded that recrystallization leads to vanishing of large consistently oriented crystallites and the formation of smaller crystallites with misaligned orientations.

This is confirmed by the results of optical observations. Figure 2, a presents a photographic image of the

Unit cell parameters of MBI · $HClO_4$ films before and after melting and recrystallization determined using the Celsiz [8] program from the analysis of X-ray diffraction patterns measured at temperature $T_{meas} = 313 \pm 1\,K$

a, Å	b, Å	c, Å	β, deg	V_{cell}, Å^3
MBI · $HClO_4$ powder [5] obtained by grinding of single crystals				
7.9123(1)*	9.9617(5)*	12.6787(3)*	95.404(1)*	994.89(6)
MBI · $HClO_4$ film/SiO_2 (quartz glass) substrate, sample No. 4 after preparation				
7.892(5)	9.974(10)	12.677(10)	95.35(6)	993.5(1.2)
MBI · $HClO_4$ film/SiO_2 (quartz glass) substrate, sample No. 3 after preparation				
7.926(13)	9.981(7)	12.736(26)	95.74(19)	1002.5(2.7)
MBI · $HClO_4$ film/SiO_2 (quartz glass) substrate, sample No. 3 after recrystallization				
7.887(5)	9.918(6)	12.624(1)	95.38(8)	983.1(1.2)
MBI · $HClO_4$/(0001) Al_2O_3 substrate, sample after preparation				
7.910(3)	9.925(11)	12.574(11)	95.34(4)	982.9(1.4)
MBI · $HClO_4$ film/(0001) Al_2O_3 substrate, sample after recrystallization				
7.898(2)	9.916(1)	12.637(4)	95.45(3)	985.2(4)

*After structure refinement by the Rietveld method.

MBI · $HClO_4$ film in the initial low-temperature phase obtained using a polarizing microscope in crossed polarizers. Films grown from solution consist of large crystallites with pronounced faceting that form a continuous coating on the substrate (Fig. 2, a). This morphology is preserved almost through to melting at T_{c1}^h. In its molten state ($T > T_{c1}^h$), the film disintegrates into droplets that wet the substrate surface. These droplets do not become transparent in crossed polarizers; i.e., they are optically isotropic.

When cooled to temperatures below T_{c1}^c, most of the droplets become transparent, indicating a transition of MBI · $HClO_4$ to an optically anisotropic intermediate phase. The phase transition to the low-temperature phase proceeds in each droplet individually at different temperatures via slow motion of the phase boundary, which transforms a textured crystalline droplet into a polycrystalline state with very small crystallites (Fig. 2, b) with the MBI · $HClO_4$ crystal symmetry at room temperature (as revealed by XRD studies; see Fig. 1, b and the table).

Figure 3, a shows the temperature dependences of capacitance of MBI · $HClO_4$ films formed on IDE/Al_2O_3 substrates at a frequency of 10 kHz subjected to heating to melting and subsequent cooling to room temperature. Photographic images of the film obtained in a polarization microscope at room temperature, in the process of heating in the melt and subsequent cooling after melting (in the intermediate phase), and again at room temperature are presented in the same figure. The transition of the film to the molten state at $T > T_{c1}^h$ is accompanied by an increase in capacitance, which grows by four orders of magnitude. In transition to the intermediate phase during cooling at $T < T_{c1}^c$, the capacitance decreases abruptly, but remains high compared to its room-temperature value. In transition to the low-temperature phase at $T < T_{c2}^c$, the capacitance and the dielectric loss tangent decrease abruptly to low levels characteristic of this phase.

Figure 3, b shows the frequency dependences of conductivity of the MBI · $HClO_4$/IDE/Al_2O_3 structure at different temperatures: in the melt ($T = 432.5$, 428, and 423.5 K) and during cooling from the melt in the intermediate phase ($T = 419$, 409.5, 400.5, and 390.5 K). As in the case of crystals, the conductivity of the structure increases during melting by approximately seven orders of magnitude (compared to the room-temperature level), and its frequency dispersion characteristic of IL manifests itself (Fig. 3, b) [9]. In the intermediate phase at $T = 390.5$ K, a weak frequency dependence of conductivity in the region up to 1000 Hz is indicative of prevalence of DC conductivity; as the frequency increases to 1 MHz, the conductivity grows due to the contribution of AC conductivity. At higher temperatures ($T = 400.5$ and 409.5 K), the DC conductivity region extends towards higher frequencies, and a region of decreasing conductivity forms at low frequencies, which is associated with near-electrode polarization induced by the concentration of ions near the electrodes. In the IL phase, the contribution of near-electrode polarization to the frequency dependences of conductivity remains significant within a wide frequency range.

Thus, it was found that an ionic liquid phase forms above the melting point in MBI · $HClO_4$ films, and a crystalline intermediate phase with its conductivity being 1–2 orders of magnitude higher than the conductivity of the low-temperature phase emerges upon cooling. The examination of the nature of this phase is of interest for further research and possible practical applications.

Acknowledgments

Conflict of interest

The authors declare that they have no conflict of interest.

References

[1] E.D. Sødahl, J. Walker, K. Berland, Cryst. Growth Des., **23** (2), 729 (2023). DOI: 10.1021/acs.cgd.2c00854

[2] W. Li, G. Tang, G. Zhang, H.M. Jafri, J. Zhou, D. Liu, Y. Liu, J. Wang, K. Jin, Y. Hu, H. Gu, Zh. Wang, J. Hong, H. Huang, L.-Q. Chen, Sh. Jiang, Q. Wang, Sci. Adv., **7** (5), eabe3068 (2021). DOI: 10.1126/sciadv.abe3068

[3] M.S. Kajamuhideen, K. Sethuraman, P. Ramasamy, J. Cryst. Growth, **483**, 16 (2018). DOI: 10.1016/j.jcrysgro.2017.11.007

[4] J. Harada, T. Shimojo, H. Oyamaguchi, H. Hasegawa, Y. Takahashi, K. Satomi, Y. Suzuki, J. Kawamata, T. Inabe, Nat. Chem., **8**, 946 (2016). DOI: 10.1038/nchem.256728

[5] E. Balashova, A. Zolotarev, A.A. Levin, V. Davydov, S. Pavlov, A. Smirnov, A. Starukhin, B. Krichevtsov, H. Zhang, F. Li, H. Luo, H. Ke, Materials, **16** (5), 1994 (2023). DOI: 10.3390/ma16051994

[6] E.V. Balashova, B.B. Krichevtsov, T.S. Kunkel, A.V. Ankudinov, J. Surf. Investig., **15** (6), 1165 (2021). DOI: 10.1134/S1027451021060057.

[7] E.V. Balashova, B.B. Krichevtsov, V.V. Lemanov, Phys. Solid State, **53** (6), 1216 (2011). DOI: 10.1134/S1063783411060047.

[8] C. Maunders, J. Etheridge, N. Wright, H.J. Whitfield, Acta. Cryst. B, **61**, 154 (2005). DOI: 10.1107/S0108768105001667

[9] J. Leys, M. Wübbenhorst, C.P. Menon, R. Rajesh, J. Thoen, C. Glorieux, P. Nockemann, B. Thijs, K. Binnemans, S. Longuemart, J. Chem. Phys., **128** (6), 064509 (2008). DOI: 10.1063/1.2827462

Translated by D.Safin